The Validity Range of LSDP Robust Controller by Exploiting the Gap Metric Theory

Ali Ameur Haj Salah, Tarek Garna, Hassani Messaoud

Abstract—This paper attempts to define the validity domain of LSDP (Loop Shaping Design Procedure) controller system, by determining the suitable uncertainty region, so that linear system be stable. Indeed the LSDP controller cannot provide stability for any perturbed system. For this, we will use the gap metric tool that is introduced into the control literature for studying robustness properties of feedback systems with uncertainty. A 2nd order electric linear system example is given to define the validity domain of LSDP controller and effectiveness gap metric.

Keywords—LSDP, Gap metric, Robust Control.

I. INTRODUCTION

THE goal of feedback is to use the principle of feedback to make the output of a dynamic process follow a desired reference accurately in spite of the external disturbances and any uncertainty in the dynamics of the process. Before the design of a feedback controller can begin, a mathematical model of the system to be controlled has to be constructed. In many cases, the modeling of complex systems is difficult, expensive and time consuming. It is impossible that mathematical model can exactly represent the behaviors of a physical system. The differences or errors between mathematical models and the physical system are generally called uncertainty. There are different methods to model the uncertainty region. Here we use additive perturbations to the nominal plant coprime factors [16]. This representation of uncertainty has no restriction on the number of right half plane poles and is capable of representing a wider class of systems. Also coprime factorizations are widely used in H_∞ optimal control theory.

The LSDP approach was firstly developed by McFarlane and Glover [13] and has been used successfully in many practical applications [1], [8], [10]. This approach is a simple and efficient robust multi-input multi-output (MIMO) controller synthesis technique that produces a controller that guarantees robust stability against normalized coprime factor uncertainty. The idea of the LSDP design is firstly to use well known loop shaping principles to introduce performance and robustness trade-offs and then, to allow the robustness optimization process to guarantee closed-loop stability.

In this paper, we determine the validity range of a robust controller determined by the LSDP approach deal with parametric uncertainty of a shaped SISO linear model $G_{sh}(s)$.

Ali Ameur Haj Salah, Tarek Garna, and Hassani Messaoud are with Electrical Department, National Engineering School of Monastir, University of Monastir, 5019 Tunisia (e-mail: aliameur@yahoo.fr, tarek.garna@ enim.rnu.tn, hassani.messaoud@enim.rnu.tn).

Indeed, for a linear model and a stabilizing controller, the stability robustness is defined as a radius of the controller as the smallest distance to a perturbation of the model which may cause the closed-loop system to become instable. Several distance notions for linear systems have been proposed, of which the so-called gap metric [17]. Then a simple and qualitative condition to verify if the LSDP controller stabilizes a perturbed model $G_{sh,\Delta}(s)$ is to check whether the gap between $G_{sh}(s)$, $G_{sh,\Delta}(s)$ is less than the stability margin. It should be clear that a perturbed model at a distance is greater than the stability margin, will be destabilized by the LSDP controller that stabilizes the linear shaped model $G_{sh}(s)$ with a stability margin equal to the gap between the two systems.

The paper is organized as follows. The LSDP approach is introduced in Section II, the gap metric theory is described in section III. Section IV presents the validity domain of LSDP controller and the effectiveness gap metric on a second-order electrical linear system.

## II. LOOP-SHAPING DESIGN PROCEDURE (LSDP)

A. Principle

The method based heavily on the loop-shaping procedure of McFarlane and Glover [12], [13] that appears in some works [5], [6], [11]. The LSDP can be divided into three distinct steps as follow:

1) Loop Shaping

Using a pre-compensator $V_1(s)$ and/or a post-compensator $V_2(s)$, the singular values of the nominal plant are shaped to give a desired open-loop shape. The nominal plant G(s) and shaping functions $V_1(s)$, $V_2(s)$ are combined to form the shaped plant, $G_{sh}(s) = V_1(s)\ G(s)\ V_2(s)$, as shown in Fig. 1. Weight selection is very important for the design. Typically, weight $V_1(s)$ and $V_2(s)$ are selected such as the open loop of the shaped plant has the following conflict properties: to achieve a good performance tracking, good disturbance rejection, large open loop gain (normally at low frequency range) is required. To achieve a good robust stability and sensor noise rejection, small open loop gain (normally at high frequency range) is required.
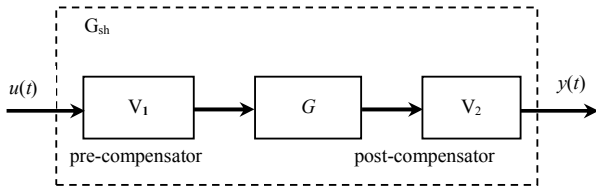
Fig. 1 Mapping Shaped plant G_{sh}

2) Robustness Verification:

We note by ε_{max} the maximum robustness margin associated with norm bounded additive uncertainties on the system's left normalized coprime factors (NCFs) [6]. If $\varepsilon_{max} \leq 0.2$ and $\varepsilon_{max} > 1$ [14], then return to step 1, adjust the weighting function $V_1(s)$ and $V_2(s)$, else we go to step 3.

3) Controller Computation and Implementation:

For $\varepsilon \leq \varepsilon_{max}$ calculate a controller $K_{\infty,opt}$ that stabilizes G_{sh} (Fig. 2). The final controller K_f for the system $G(s)$ is constructed by combining the controller $K_{\infty,opt}$ with the shaping functions $V_1(s)$ and $V_2(s)$ such that $K_f(s) = V_1(s) K_{\infty,opt}(s) V_2(s)$. The controller $K_{\infty,opt}(s)$ is presented in the next section.
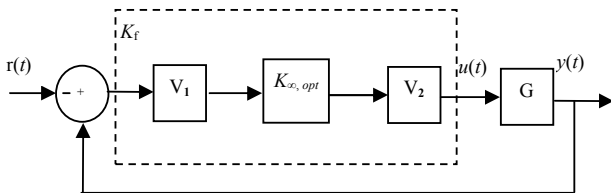
Fig. 2 Controller for system G(s)

B. Optimal Dynamic Controller $K_{\infty,opt}$ Computation

Consider the strictly proper state space representation of the open loop shaped plant G_{sh}:

$$G_{sh}: \begin{cases} \dot{x} = A_{sh}x + B_{sh}u \\ y = C_{sh}x \end{cases} \quad (1)$$

where x is the state, y and u are the output and the input respectively and A_{sh}, B_{sh} and C_{sh} are matrices of the shaped plant in state-space representation. The $K_{\infty,opt}$ controller is given by the transfer matrix [7]:

$$K_{\infty,opt} := \left[\begin{array}{c|c} A_{sh} - B_{sh}B_{sh}^T X + \varepsilon_{max}^{-2} W^{-1} Z C_{sh}^T C_{sh} & \varepsilon_{max}^{-2} W^{-1} Z C_{sh}^T \\ \hline B_{sh}^T X & 0 \end{array} \right] \quad (2)$$

where W is given by: $W = (I + X Z - (\varepsilon_{max})^{-2} I)^T$ and the matrices X and Z solve the control (respectively filtering) algebraic Riccati equations (CARE, FARE):

$$CARE: A_{sh}^T X + X A_{sh} - X B_{sh}B_{sh}^T X + C_{sh}^T C_{sh} = 0$$

$$FARE: A_{sh}^T Y + A_{sh}Z - Z C_{sh}^T C_{sh} Z + B_{sh} B_{sh}^T = 0 \quad (3)$$

The robust controller $K_{\infty,opt}$ can be solved by MATLAB@ with function 'coprimeunc' of the Robust Control toolbox. Additionally it computes the corresponding maximum robustness margin ε_{max} from:

$$\varepsilon_{max} = (1 + \rho(XZ))^{-1/2} \quad (4)$$

where ρ denotes the spectral radius.

III. GAP METRIC THEORY

Before the gap metric was introduced in [17] to study the robustness of feedback systems subject to modeling uncertainty, several authors developed computational tools notably in [2]-[4], [18] for a fairly general class of infinite-dimensional systems. In [2], the authors show that the feedback optimization in the gap metric is equivalent to feedback optimization with respect to normalized factor perturbations. El-Sakkary [15] shows that the gap metric is better suited to measure the distance between two linear systems than a metric based on norms. Gap metric denoted by $\delta_g(G_{sh}, G_{sh,\Delta})$ introduces the notion of "distance" between two nominal system model G and a perturbed model $G_{sh,\Delta}$ as the "gap" between their graphs. The calculation of the gap metric begins with two finite dimensional linear systems with the same number of inputs and outputs that left normalized coprime factorizations are given by:

$$G_{sh} = \tilde{M}^{-1} \tilde{N}, G_{sh,\Delta} = (\tilde{M} + \Delta_{\tilde{M}})^{-1} (\tilde{N} + \Delta_{\tilde{N}}) \quad (5)$$

$\tilde{M}$ and $\tilde{N}$ ($\in RH_\infty$) denote the left factors of the nominal system model G, $\Delta_{\tilde{M}}$ and $\Delta_{\tilde{N}}$ ($\in RH_\infty$) model the uncertainty of right coprime factors of G with $\| [\Delta_{\tilde{M}} \ \Delta_{\tilde{N}}] \|_\infty < \varepsilon$. It can be shown that the gap metric can be computed using the projection operators or the coprime factorizations [15]:

$$\delta_g(G_{sh}, G_{sh\Delta}) = \sup \left\{ \inf_{Q \in \Re H_\infty} \left\| \begin{bmatrix} \tilde{M} \\ \tilde{N} \end{bmatrix} - \begin{bmatrix} \tilde{M} + \Delta_{\tilde{M}} \\ \tilde{N} + \Delta_{\tilde{N}} \end{bmatrix} Q \right\|_\infty, \inf_{Q \in \Re H_\infty} \left\| \begin{bmatrix} \tilde{M} + \Delta_{\tilde{M}} \\ \tilde{N} + \Delta_{\tilde{N}} \end{bmatrix} - \begin{bmatrix} \tilde{M} \\ \tilde{N} \end{bmatrix} Q \right\|_\infty \right\} \quad (6)$$

The gap metric can be calculated to any desired accuracy by using MATLAB@ Robust Control Toolbox and the command `gap metric'. The connection between the gap metric theory and LSDP approach of section 2 is due to Georgiou and Smith [2]. The following theorem [2] gives necessary and sufficient conditions for the gap between G_{sh} and $G_{sh,\Delta}$ on the one hand and, on the other hand, the extent that a controller $K_{\infty,opt}$ stabilizes a right coprime factor perturbed plant $G_{sh,\Delta}$ given that it robustly stabilizes a nominal plant G_{sh}.

Theorem 1[2]. *Consider a shaped model G_{sh} with a left normalized coprime factorization $G_{sh} = \tilde{M}^{-1} \tilde{N}$ and a controller $K_{\infty,opt}$ that stabilizes it. Take a real number ε_{max} so that $0 \leq \varepsilon_{max} \leq 1$. Then, these two statements are equivalent:*
a. *The closed loop pair $[G_{sh,\Delta}, K_{\infty,opt}]$ is stable for every uncertain model $G_{sh,\Delta}$ with $G_{sh,\Delta} = (\tilde{M} + \Delta_{\tilde{M}})^{-1} (\tilde{N} + \Delta_{\tilde{N}})$ where $\Delta_{\tilde{M}}$ and $\Delta_{\tilde{N}}$ ($\in \Re H_\infty$) and $\| [\Delta_{\tilde{M}} \ \Delta_{\tilde{N}}] \| < \varepsilon_{max}$.*
b. *The closed loop pair $[G_{sh,\Delta}, K_{\infty,opt}]$ is stable for every model $G_{sh\Delta}$ for which $\delta_g(G_{sh}, G_{sh,\Delta}) < \varepsilon_{max}$* ∎

IV. SIMULATION EXAMPLE: 2ND ORDER ELECTRIC LINEAR SYSTEM

We consider a 2nd order linear electrical system represented by the following electric circuit:

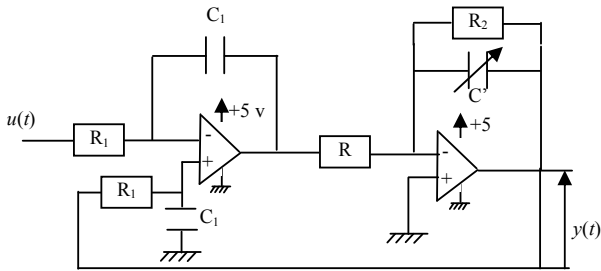Fig. 3 Second order electric linear system circuit

With $R_1 = R = R_2 = 68$ KΩ, $C_1 = 10$ nF and C' a variable capacity. The system is defined by the following transfer function:

$$G(s) = \frac{R_2}{R\,R_1\,R_2\,C_1\,C'\,s^2 + R\,R_1\,C_1\,s + R_2} \quad (7)$$

or yet canonical form:

$$G(s) = \frac{k\;w_0^2}{s^2 + 2\;m\;w_0\;s + w_0^2} \quad (8)$$

as:

- *K* the static gain:

$$k = 1 \quad (9)$$

- w_0 the natural frequency

$$w_0 = \sqrt{\frac{1}{R\,R_1\,C_1\,C'}} \quad (10)$$

- *m* the damping ratio

$$m = \frac{1}{2\,R_2}\sqrt{\frac{R\,R_1\,C_1}{C'}} \quad (11)$$

For the nominal representation G(s) we set:

$$C' = C_0' = 0.033\ 10^{-8}\ \text{F} \quad (12)$$

and G(s) can be written as:

$$G(s) = \frac{68000}{(s + 1522.6)\,(s + 43041)} \quad (13)$$

For the weighted representation $G_{sh}(s)$ we choose the weighting functions $V_1(s)$ and $V_2(s)$ as:

$$\begin{cases} V_1(s) = \dfrac{3}{(s + 0.01)} \\ V_2(s) = 1 \end{cases} \quad (14)$$

The filter can increase the gain in low frequencies and reduce the gain at high frequencies. As a result, G_{sh} (s) is written:

$$G_{sh}(s) = \frac{2.04\ \ 10^5}{1.038\ 10^{-3}\ s^3 + 46.24\ s^2 + 68\ \ 10^3\ \ s + 680} \quad (15)$$

From (15) the transfer matrix G_{sh} (s) is defined by the following state-space matrix A_{sh}, B_{sh}, C_{sh} and D_{sh}:

$$A_{sh} = 10^4 \begin{bmatrix} -4.4563 & -0.8 & -0.001 \\ 0.8192 & 0 & 0 \\ 0 & 0.0008 & 0 \end{bmatrix} \quad B_{sh} = \begin{pmatrix} 64 \\ 0 \\ 0 \end{pmatrix} \quad (16)$$

$$C_{sh} = \begin{pmatrix} 0 & 0 & 46.8737 \end{pmatrix} \quad D_{sh} = 0 \quad (17)$$

By applying the H_∞ loop shaping method, the robustness margin ε_{max} is founded at 0.7006 from (4). This value indicates that the selected weighting function is compatible with the robust stability requirement. Based on the conventional technique presented in Section II, the conventional H_∞ loop shaping controller is synthesized as:

$$K_{\infty,opt}(s) = \frac{151.2\ s^2 + 6.74\ 10^6\ s + 9.911\ 10^9}{s^3 + 4.472\ 10^4\ s^2 + 7.242\ 10^7\ s + 1.016\ 10^{10}}. \quad (18)$$

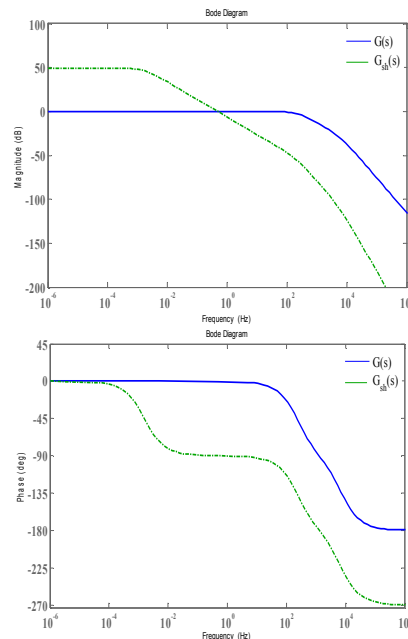We represent, the bode diagrams of G(s) and $G_{sh}(s)$ in Fig. 4:

Fig. 4 Bode diagrams of G(s) and $G_{sh}(s)$

To test the performance of the $K_{\infty,opt}$ robust controller to guarantee the robust stabilization of shaped closed loop system $G_{sh}(s)$ over parametric uncertainties, we propose to disturb the nominal model $G(s)$ by varying the capacitance value C_0'. This variation results from an added parametric uncertainty to the value of C_0' as:

$$C'(\Delta_{C'}) = C_0' + \Delta_{C'} \quad / \quad C_0' = 0.033 \cdot 10^{-8}\,F \quad and \quad \Delta_{C'} > 0 \quad (19)$$

As a result, from (4) we get the uncertain system $G_{\Delta c'}(s)$:

$$G_{\Delta_{C'}}(s) = \frac{k\ w_{0,\Delta_{C'}}^2}{s^2 + 2\ m_{\Delta_{C'}}\ w_{0,\Delta_{C'}}\ s + w_{0,\Delta_{C'}}^2} \quad (20)$$

with:

$$w_{0,\Delta_{C'}} = \sqrt{\frac{1}{R\,R_1\,C_1\,(C_0' + \Delta_{C'})}} \quad (21)$$

$$m_{\Delta_{C'}} = \frac{1}{2\,R_2}\sqrt{\frac{R\,R_1\,C_1}{(C_0' + \Delta_{C'})}} \quad (22)$$

Also we obtain the following uncertain shaped representation $G_{sh,\Delta c'}(s)$ as:

$$G_{sh,\Delta_{C'}}(s) = V_1(s)\ G_{\Delta_{C'}}(s)\ V_2(s) \quad (23)$$

In order to test the stability margin $G_{sh,\Delta c'}(s)$ in terms of the parametric uncertainty $\Delta_{c'}$ we represent in Figs. 5 and 6 the evolution of the corresponding gain and phase margins (Mg, Mφ). From these figures, we see that the uncertain shaped model becomes unstable for $\Delta_{c'} \geq 0.4902 \cdot 10^{-5}$ F since Mφ $(G_{sh,\Delta c'}) \leq -0.036°$ and Mg $(G_{sh,\Delta c'}) \approx 0$ dB. It is interesting therefore to determine the range variation of the uncertainty parameter $\Delta_{c'}$ in which the robust controller $K_{\infty,opt}$ guarantees the robust stabilization of uncertain shaped system $G_{sh,\Delta c'}(s)$. In this case, using the gap metric theory we propose to quantify from (6) the distance between the shaped system G_{sh} and the uncertain shaped system $G_{sh,\Delta c'}$ relative to the maximum stability margin ε_{max}. This is illustrated in Fig. 8 plotting the variation of the gap metric δg $(G_{sh},\ G_{sh,\Delta c'})$ as functions of $\Delta_{c'}$ as δg $(G_{sh},\ G_{sh,\Delta c'}) \leq \varepsilon_{max}$.
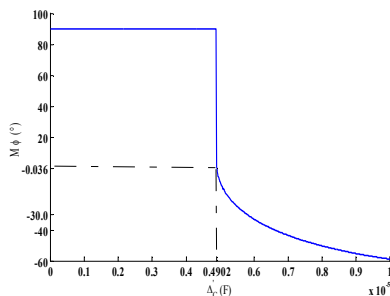

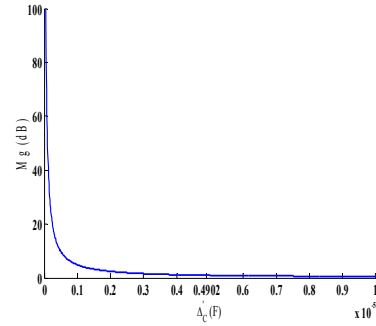Fig. 5 Evolution of Mφ $(G_{sh,\Delta c'})$ as function of $\Delta_{c'}$

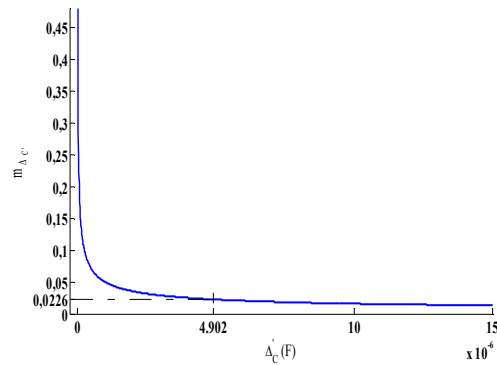Fig. 6 Evolution of Mg $(G_{sh,\Delta c'})$ as function of $\Delta_{c'}$

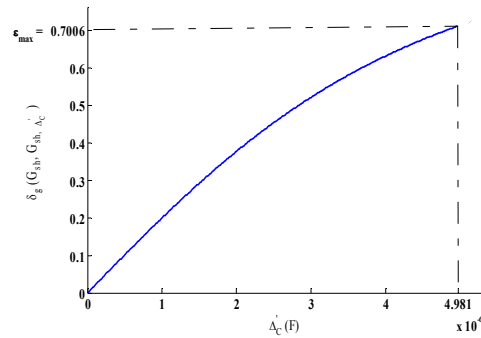Fig. 7 Evolution of $m_{\Delta c'}$ as function of $\Delta_{c'}$

Fig. 8 Evolution of δg $(G_{sh},\ G_{sh,\Delta c'})$ as function of $\Delta_{c'}$

From Fig. 8, it may be observed that the limit value δg $(G_{sh}, G_{sh,\Delta c'}) = \varepsilon_{max}$ is surpassed at $\Delta_{c'} = 0.498 \cdot 10^{-5}$ F. This value is above $\Delta_{c'} = 0.4902 \cdot 10^{-5}$ F that characterizes the instability of uncertain shaped system $G_{sh,\Delta c'}$. In Table I, we summarize for three values $\Delta_{c'}$, $\Delta_{c'} = 4.6775 \cdot 10^{-9}$ F, $\Delta_{c'} = 10^{-6}$ F and $\Delta_{c'} = 0.494 \cdot 10^{-5}$ F performance for corrected system by open loop robust controller $K_{\infty,opt}$ in terms of:

- Gap metric δg $(G_{sh},\ G_{sh,\Delta c'})$
- Phase margin Mφ $(K_{\infty,opt}\ G_{sh,\Delta c'})$.
- Gain margin Mg $(K_{\infty,opt}\ G_{sh,\Delta c'})$.

We propose to compare the closed loop performance correction $K_{\infty,opt}$ with respect to the following classical PID control

$$C(s) = K_p + \frac{K_i}{s} + K_d \frac{s}{(N^{-1} s + 1)} \qquad (24)$$

where $N = 3632.7536$, $K_p = 1.8417$, $K_i = 8.2761$ and $K_d = -0.0003$. In Figs. 9-20 are shown the reference, the output and the input signals using the robust controller $K_{\infty,opt}$ and the classical PID control considering $\Delta_{c'} = 4.6775\ 10\text{-}9$ F , $\Delta_{c'} = 10^{-6}$ F and $\Delta_{c'} = 0.494\ 10^{-5}$ F. In addition, it is proposed to test the performance of the robust controller $K_{\infty,opt}$ for $\Delta_{c'}$ change over time as $0 \le \Delta_{c'}(t) \le 2\ 10^{-5}$ F. This variation is defined by (25) and shown in Fig. 21. So, we track in Figs. 22 and 23 the input and output signals evolution respectively in the presence of the controller $K_{\infty,opt}$.

$$\Delta_{C'}(t) = 10^{-5} \left(1 + sin(0.15\ \pi\ t)\ cos(0.6\ \pi\ t) \right) \qquad (25)$$

TABLE I
ROBUST CONTROLLER PERFORMANCE

	$\Delta_{c'}$	$4.6775\ 10^{-9}$F	10^{-6} F	$0.494\ 10^{-5}$ F
	$C'(\Delta_{c'})$	$5.0075\ 10^{-9}$ F	10^{-6} F	$0.494\ 10^{-5}$ F
Gap metric	$\delta g\ (G_{sh},\ G_{sh,\Delta c'})$	$9.7559\ 10^{-4}$	0.199	0.7003
Phase margin	$M\varphi\ (K_{\infty,opt}\ G_{sh,\Delta c'})$	$89\ °$	$89\ °$	$89\ °$
Gain margin	$Mg\ (K_{\infty,opt}\ G_{sh,\Delta c'})$	54 dB	18.4 dB	1.41 dB

$K_{\infty,opt}$ Robust Controller for $\Delta_{c'} = 4.6775\ 10^{-9}$ F

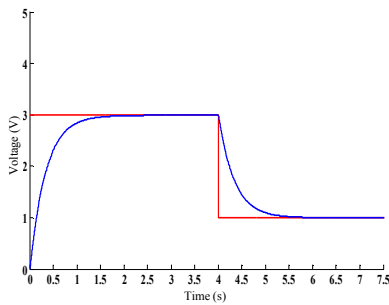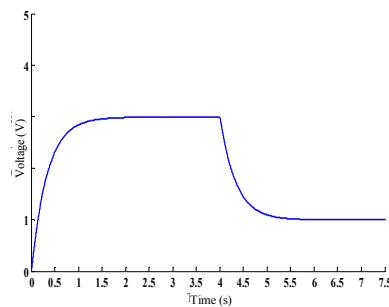Fig. 9 Evolution of the output signal $y(t)$ and reference r(t) for $\Delta_{c'} = 4.6775\ 10^{-9}$ F

Fig. 10 Evolution of input signal $u(t)$ for $\Delta_{c'} = 4.6775\ 10^{-9}$ F

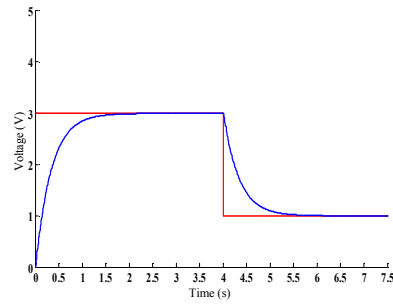$K_{\infty,opt}$ Robust Controller for $\Delta_{c'} = 10^{-6}$ F

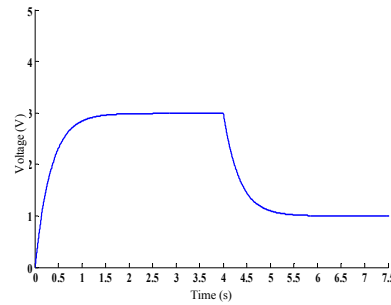Fig. 11 Evolution of the output signal $y(t)$ and reference r(t) for $\Delta_{c'} = 10^{-6}$ F

Fig. 12 Evolution of input signal $u(t)$ and reference r(t) for $\Delta_{c'} = 10^{-6}$ F

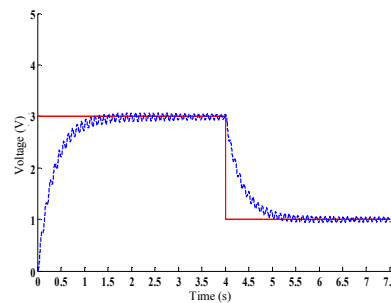$K_{\infty,opt}$ Robust Controller for $\Delta_{c'} = 0.494\ 10^{-5}$ F

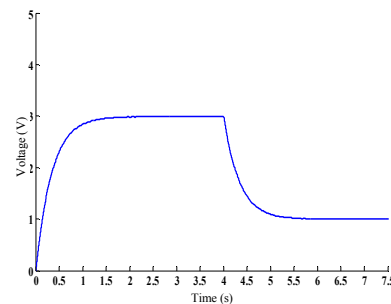Fig. 13 Evolution of output signal $y(t)$ and reference r(t) for $\Delta_{c'} = 0.494\ 10^{-5}$ F

Fig. 14 Evolution of input signal $u(t)$ for $\Delta_{c'} = 0.494\ 10^{-5}$ F

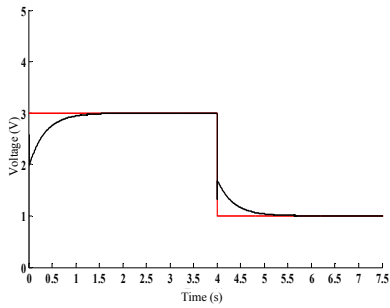PID Controller for $\Delta_{c'} = 4.6775 \ 10^{-9}$ F

Fig. 15 Evolution of the output signal $y(t)$ and reference $r(t)$ for $\Delta_{c'} = 4.6775 \ 10^{-9}$ F
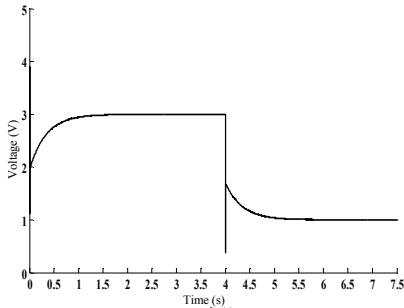

Fig. 16 Evolution of the input signal $u(t)$ for $\Delta_{c'} = 4.6775 \ 10^{-9}$ F

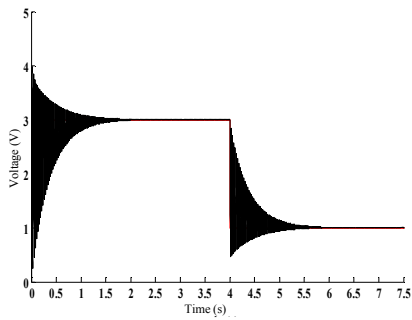PID Controller for $\Delta_{c'} = 10^{-6}$ F

Fig. 17 Evolution of the input signal $u(t)$ for $\Delta_{c'} = 4.6775 \ 10^{-9}$ F
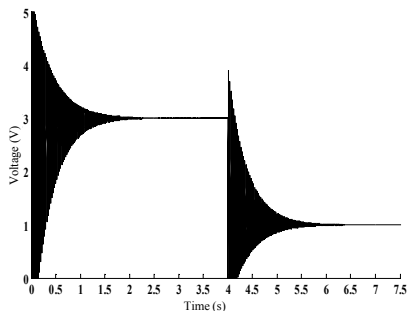

Fig. 18 Evolution the input signal $u(t)$ for $\Delta_{c'} = 10^{-6}$ F

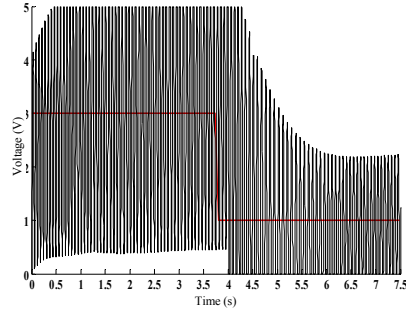PID Controller for $\Delta_{c'} = 0.494 \ 10^{-5}$ F

Fig. 19 Evolution of the output signal $y(t)$ for $\Delta_{c'} = 0.494 \ 10^{-5}$ F
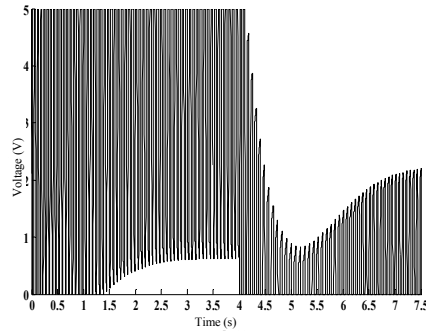

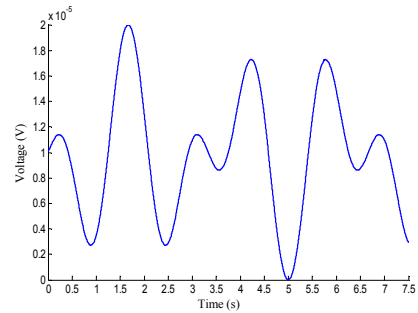Fig. 20 Evolution of the input signal $u(t)$ for $\Delta_{c'} = 0.494 \ 10^{-5}$ F
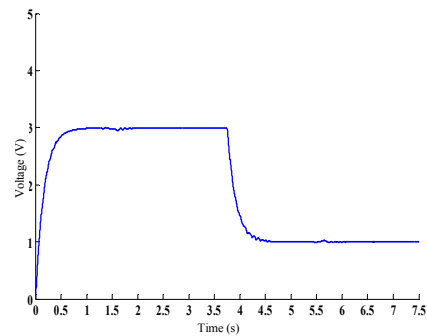

Fig. 21 Evolution of $\Delta_{c'}(t)$

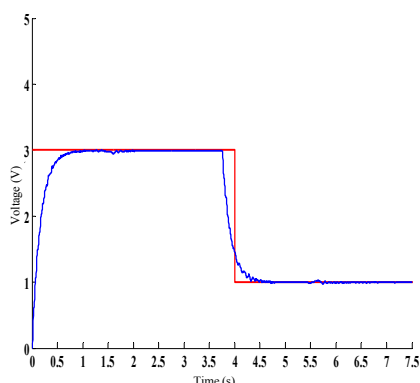Fig. 22 Evolution of the input signal $u(t)$ for $1.6941 \ 10^{-21} \leq \Delta_{c'} \leq 2 \ 10^{-5}$ F

Fig. 23 Evolution of the output signal $y(t)$ a reference r(t) for 1.6941 $10^{-21} \leq \Delta_{c'} \leq 2\ 10^{-5}$ F

The simulation and experimental results showed that the robustness and efficiency of the robust controller $K_{\infty,opt}$ was gained when compared with the classical PID control. Indeed in Figs. 15-20 shown performance of PID controller present oscillations that are amplified as and as we increase the value of the parameter uncertainty $\Delta_{c'}$. This is explained by the reduction of the damping coefficient $m_{\Delta c'}$ increasing $\Delta_{c'}$ because uncertain system $G_{\Delta c'}(s)$ becomes increasingly oscillating and approaching instability. Indeed, from (22) the value of $m_{\Delta c'}$ changes from 0.7066 for $\Delta_{c'}= 4.6775\ 10^{-9}$ F to 0.05 for $\Delta_{c'} = 10^{-6}$ F and then to 0.0225 for $\Delta_{c'}= 0.494\ 10^{-5}$ F. However the performance and robustness of LSDP controller is significantly more authoritative than classical PID control system design. Indeed, we see from Figs. 11 and 12 are small oscillations, and from Figs. 10, 12 and 14, the input signal shows no saturation.

From Table I, the $K_{\infty,opt}$ robust controller stabilizes $G_{sh,\Delta c'}(s)$ near the zone of instability characterized for $\Delta_{c'} \geq 0.4902\ 10^{-5}$ F. Indeed, for $\Delta_{c'} = 0.494\ 10^{-5}$ F and from Table I, we get through the corrector $K_{\infty,opt}$ margin phase Mφ ($K_{\infty,opt}\ G_{sh,\Delta c'}$) = 89° and margin gain Mg ($K_{\infty,opt}\ G_{sh,\Delta c'}$) = 1.41 dB. In addition, we note that these performances stability are immediately taking into account the gap metric theory. Indeed, when the shaped system $G_{sh}(s)$ is unstable, we have in Fig. 8 for $\Delta_{c'}$ = 0.494 10^{-5} F a gap metric δg (G_{sh}, $G_{sh,\Delta c'}$) = ε_{max}. That is to say from the result b of Theorem 1, the $K_{\infty,opt}$ robust controller stabilizes the $K_{\infty,opt}$ uncertain system checking δg (G_{sh}, $G_{sh,\Delta c'}$) $\leq \varepsilon_{max}$.

V.CONCLUSION

In this paper, we have shown that for a linear system, the validity of the LSDP approach to maintain the desired robustness depends on uncertainty domain as-well defined. The latter is obtained by calculating the gap metric between the nominal linear system and the corresponding perturbed system, depending on the robust margin calculated by LSDP approach. Indeed, a simple and qualitative condition to verify if the LSDP controller stabilizes a perturbed model is to check whether the gap between the two systems is less than the stability margin. Finally, we have shown the robustness and efficiency of the LSDP robust controller is gained when compared with the classical PID controller.

REFERENCES

[1] SL. Ballois, G. Duc, "H_∞ control of a satellite axis: Loop shaping, controller reduction, and μ-analysis". contr Eng Practice 1996; 4 (7): 1001-7
[2] Georgiou, T.T., and M. Smith, "Optimal Robustness in the Gap Metric". IEEE Transactions on Automatic Control, 35(6):673-686, 1990.
[3] Georgiou,T.T., "On the computation of the gap metric". Systems Control Letters, vol. 11, 1988, p. 253–257.
[4] Georgiou,T.T and M. Smith, "Robust stabilization in the gap metric: controller design for distributed plants". IEEE Trans. Automat. Control 37 (8) (1992) 1133–1143.
[5] K. Glover, "All optimal Hankel-norm approximations of linear multivariable systems and their L$_\infty$-error bounds". International Journal of Control, 39(6), (1984) 1115- 93.
[6] K. Glover and D. McFarlane, "Robust stabilization of normalized coprime factor plant descriptions with H_∞-bounded uncertainty". IEEE Transactions on Automatic Control, vol. 34, pp. 821-830, 1989.
[7] K. Glover and J. Doyle, "State-Space Formulae for all Stabilizing Controllers that Satisfy an H$_\infty$-Norm Bound and Relations to Risk Sensitivity". Systems & Control Letters, 11:167- 172, 1988.
[8] K. Glover, AP. Dowling, "Control of combustion oscillations via H_∞ loop shaping, μ-analysis and integral quadratic constraints". Automatica 2003; 39(2): 219-31.
[9] J. Jayender, RV. Patel, S. Nikumb, M. Ostojic, "H_∞loop shaping controller for shaped memory alloy actuators". In: Proceedings of the IEEE conference on decision and control, 2005, p. 653-8.
[10] S. Kaitwanidvilai, M. Parnichkun, "Genetic algorithm-based fixed-structure robust H_∞ loop shaping control of a pneumatic servo system". J Robot Mechatron 2004; 16 (4): 362-73.
[11] D. Limebeer and M. Green, "Linear Robust Control". Prentice-Hall, 1996.
[12] D. McFarlane and K. Glover, "Robust Controller Design using Normalized Coprime Factor Plant Descriptions". Lecture Notes in Control and Information Science. Springer Verlag, Berlin, 1990.
[13] D. McFarlane and K. Glover, "A Loop Shaping Design Procedure Using H_∞ Synthesis". IEEE Transactions on Automatic Control, 37(6):759-769, 1992.
[14] S. Skogestad, I. Postlethwaite, "Multivariable feedback control: Analysis and design". John Wiley & Sons, 2005.
[15] EL-Sakkary A.K, "The gap metric: Rbustness of stabilization of feedback system,"IEEE Trans.Automat.contr., vol.AC-30, pp.240-247, Mar.1985.
[16] M. Vidyasagar and H. Kimura, "Robust controllers for uncertain linear multivariable systems". Automatica, 22:85-94, 1986.
[17] G. Zames and A.K. El-Sakkary, "Unstable systems and feedback: the gap metric". in: Proceedings of the Allerton Conference, 1980, pp. 380–385.
[18] S.Q. Zhu, M.L.J. Hautus, C. Praagman, "Sufficient conditions for robust BIBO stabilisation: given by the gap metric". Systems Control Lett. 11 (1988) 53–59.